



## The Influence of PO<sub>4</sub> to Bio-silica Catalyst on Synthesis Benign Additive Fuel



D. Radwan<sup>1</sup>, T. Zaki<sup>1,2</sup>, H. M. Abd El Salam<sup>3</sup>, D. Aman<sup>1\*</sup>

<sup>1</sup>Department of Refining, Egyptian Petroleum Research Institute (EPRI), Nasr city, PO Box 11727, Cairo, Egypt

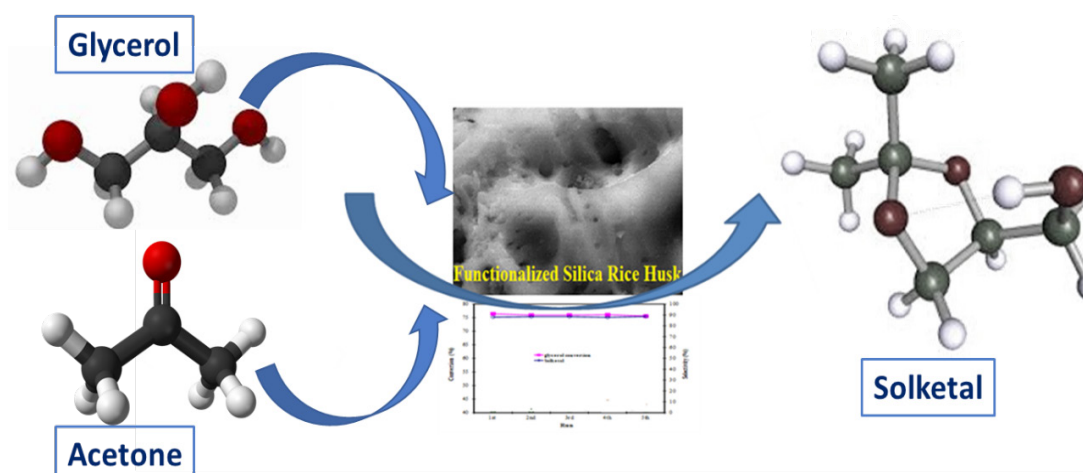
<sup>2</sup>EPRI-Nanotechnology Center, Egyptian Petroleum Research Institute, Nasr City, PO Box 11727, Cairo, Egypt

<sup>3</sup>Analysis and Evaluation Division, Egyptian Petroleum Research Institute, Nasr City, PO Box 11727, Cairo, Egypt.

**F**UEL additive solketal can be produced through acetalization reaction of biodiesel by-product (glycerol) and acetone. This reaction was conducted over acidified silica derived from sustainable bioresource rice husk in a batch reactor under the solvent-free condition. The chemical and structural properties of the prepared catalyst were studied by X-ray diffraction (XRD), Fourier transforms infrared spectroscopy (FTIR), N<sub>2</sub> adsorption/desorption isotherms, temperature-programmed desorption of ammonia (NH<sub>3</sub>-TPD) and scanning electron microscope (SEM). Based on this paper, the optimized conditions using 15% phosphoric acid acidified silica extracted from rice huskash (10 wt.% PO<sub>4</sub> loaded SiO<sub>2</sub>) are 50°C (lower temperature) with the molar ratio of acetone: glycerol = 2. Reusability test used to examine the stability of the catalytic activity was investigated. This effort is a serious step for development and taking apart of solketal as the main product from glycerol and acetone by using waste resources.

**Keywords:** Silica, Acidic, Solketal, Renewable resources, Rice husk, Glycerol, Acetone.

### Graphical Abstract



\*Corresponding author e-mail: delvin.aman@epri.sci.eg

Received 11/07/2019; Accepted 20/08/2019

DOI: 10.21608/ejchem.2019.14728.1890

© 2020 National Information and Documentation Center (NIDOC)

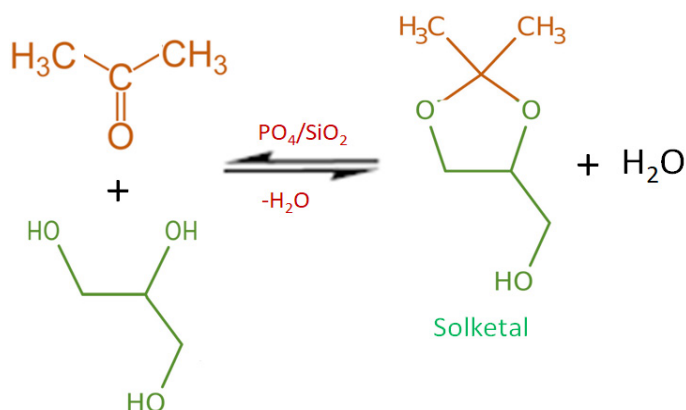
## Introduction

As a sustainable bioresource, biomass has concerned attention to preparing of highly developed materials for different applications, attributable to their low value, their abundance particularly in rice-producing countries like Egypt, their speedy regeneration and being friendly in respect to the environment. In the rice milling industry, rice husks are by-products of huge amount in the world ( $\sim 2.9 \times 10^7$  t annually). It mainly consists of organic materials like hemicellulose, cellulose, and lignin (75-90 wt.%). The ash (17–20 wt.%) produce by burning the husk underneath controlled conditions including high pure silicon oxide, that represents 90 wt.% of that ash. Consequently, the husks of rice are reconsidered as natural stocks to prepare for silica-based adsorbents or catalyst supports [1- 3]. The biodiesel, the future's fuel, has been considered as a decent alternative for fossil fuels, like diesel. Recently, numerous studies have been given to this renewable fuel [4-6]. However, the low cost of diesel and the expanding cost of the source oils for biodiesel production had been considered as challenges. It is then important to enhance the financial plausibility of biodiesel production by the increase of value-added of by-products such as glycerol, which are formed during the biodiesel production [7]. The glycerol is catalytically converted for produce the intermediates chemicals such as solvents, and additives, like 1,3-propanediol, 1,2-propanediol [8], polyglycerols [9], di- and tri-acetyl glycerol esters [10], 3-hydroxypropionaldehyde [11], acrolein [12], and solketal [13]. The solketal (2,2-dimethyl 1,3-dioxolane-4-methanol), which is the product of the catalytic reaction of glycerol and acetone, has a significant function which used to enhance transportation fuel quality (in

the additive form), in the polymer industry (as a plasticizer) also in the pharmaceutical industry (as a solvent) [14].

The addition of the solketal to diesel fuel motors reduces the carbon monoxide, hydrocarbons and unregulated aldehydes emissions. Also, it used as cold flow improver for biodiesel fuel. Blending the solketal with standard gasoline fuel (1-5 vol. %) reduces the gum formation and consequently improves the octane number [15]. From environmental sight, it is less toxicity fuel additive than the traditional one, Methyl tert-butyl ether (MTBE) [16]. Regarding the conventional catalytic production of solketal, inorganic acids such as  $H_2SO_4$ ,  $H_3PO_4$  or HCl are usually used. This, in turn, can lead to cause environmental problems because of using toxic materials, elimination of the effluents and serious erosion of devices. In the industrial procedures in last year's, heterogeneous solid acid catalysts, including Amberlyst resins [17], mixed oxides [18], niobia [19], zirconia [20] and functionalized activated carbons [21,22], have the perspective to use rather than this dangerous catalyst (liquid acid). Also, solid catalysts can reuse for several runs after easy separation methods like filtration or centrifugation [23-25].

During this work, the catalytic acetalization of the glycerol with acetone (Scheme 1) was investigated using phosphate silica derived from sustainable bioresource rice husk under the solvent-free condition. The catalyst was characterized by different physicochemical characterizations techniques for verifying the catalyst properties. Also, the effective acetalization variables such as different reaction temperatures, acetone: glycerol molar ratios, and weight of catalyst used during the reaction are studied in detail.



Scheme 1. Acetalization of glycerol with acetone .

## Experimental

### *Extracted silica from the rice husk*

Dry the raw rice husk obtained from Egyptian agricultural field (Kafr El-Shaikh) was sieved to a grain diameter of less than 0.5 mm. The raw husk was carefully rinsed with distilled water, filtered and then dried in the oven at 110°C. The dried rice husk (100 g) placed in a ceramic tube and introduced into a muffle furnace where the pyrolysis step was performed under nitrogen flow (10 ml/min). The temperature was raised with ramping with 5°C/min till 700°C. The samples were held at this pyrolysis temperature for 4 h.

### *Preparation of phosphate silica*

Acidified silica by phosphoric acid (10 wt.% PO<sub>4</sub> loaded SiO<sub>2</sub>) prepared by acidification silica using H<sub>3</sub>PO<sub>4</sub> solution (15 wt%). That treated silica dried at 120°C up to 12 h and subsequently was heated in purified nitrogen with the flow (10 ml/min) at 530°C for 3 h.

### *Characterization of the materials*

X-ray powder diffraction Analysis (XRD) performed out using Shimadzu XD-1 diffractometer in 2θ = 20-80°. The spectra of Fourier Transform Infrared Spectroscopy (FTIR) were verified by a Nicolet 740 FTIR spectrometer under ambient conditions by using KBr disks for averaging 100 spectra with a nominal resolution of 4 cm<sup>-1</sup>. Surface properties of the prepared materials were characterized by Quantachrome NOVA2000 at low temperature (-196°C) through N<sub>2</sub> adsorption-desorption isotherms and measuring the pore size distribution. Before adsorption measurements, the samples were evacuated at 350°C for over night. Temperature programmed desorption of ammonia (NH<sub>3</sub>-TPD) was carried out in automatic equipment (Chem BET 3000, Quantachrome). The microscopic characteristic by scanning electron microscope (SEM) of silica ex rice husk ash and phosphoric acidification silica texture are examined using a JEOL JSM-5300 scanning electron microscope.

### *Catalytic reaction*

Glycerol catalytic acetalization was performed in a batch reactor containing a round bottom flask with a reflux condenser at temperatures ranging from 50, 70 and 100°C and an acetone/glycerol ratio of 2, 4 and 6 mol/mol. Typical acetalization reactions were performed by the magnetically stirring of 100-700 mg for one hour. Also, the stability of the catalysts for 6 hours was studied. The solvent used to wash catalyst every run

is acetone. After the certain reaction time, a segment of the reaction mixture was taken apart by centrifugation, which was analyzed by a GC equipped with a wax capillary column called a BP-20 and analyzing using a flame ionization detector (FID). The catalyst recyclability was studied via reused spend catalyst five times. After each run, the catalyst powder was separated from the reaction mixture by centrifuge, rinsed thoroughly and dried, before reusing. The conversion of glycerol and the selectivity to solketal were estimated using these following equations:

$$\text{Conversion}\% = \frac{G_i - G_f}{G_i} \times 100$$

$$\text{Selectivity}\% = \frac{S_p}{G_i - G_f} \times 100$$

Where as,  $G_i$ ,  $G_f$  and  $S_p$  were the initial and final moles value of glycerol and produced solketal in the reaction medium, respectively.

## Results and Discussion

The XRD patterns of extracted silica from rice husk and acidified one are shown in Fig. 1. The patterns of both samples are similar. As detected the very broad peaks at 2θ = 22° are a characteristic peak of silica which authenticated its nature amorphous [1]. This elucidates that crystallization of silica did not format that pyrolysis temperature (700°C for 4h), Acidified silica with phosphoric acid, which was heated at 530°C demonstrated an exceedingly broad peak in the 2θ range from 15° to 30°, which representative for amorphous silica phase, and no detectable peak for PO<sub>4</sub>/SiO<sub>2</sub> in the pattern. That is meaning well dispersion of phosphoric acid over silica surface which may cause some deformation of silica phase to create catalytic active sites.[26].

The FTIR spectrums of the obtained parent silica and phosphate silica are given in (Fig. 2 a and b). The characteristic bands of the asymmetric and symmetric stretching vibrations of the Si-O-Si at 1055 and 800 cm<sup>-1</sup>, successively. The bending vibrations of the adsorbed and coordinately bound water appeared at 1635 and 3450 cm<sup>-1</sup>, respectively [27]. On the other hand, the FTIR spectrum of the phosphate silica (PO<sub>4</sub>/SiO<sub>2</sub>) showed a shoulder of frequencies around 1030 cm<sup>-1</sup>, which featured to the stretching mode of PO<sub>4</sub><sup>-3</sup> vibration indicating the formation of acidified silica PO<sub>4</sub>/SiO<sub>2</sub>[8, 28].

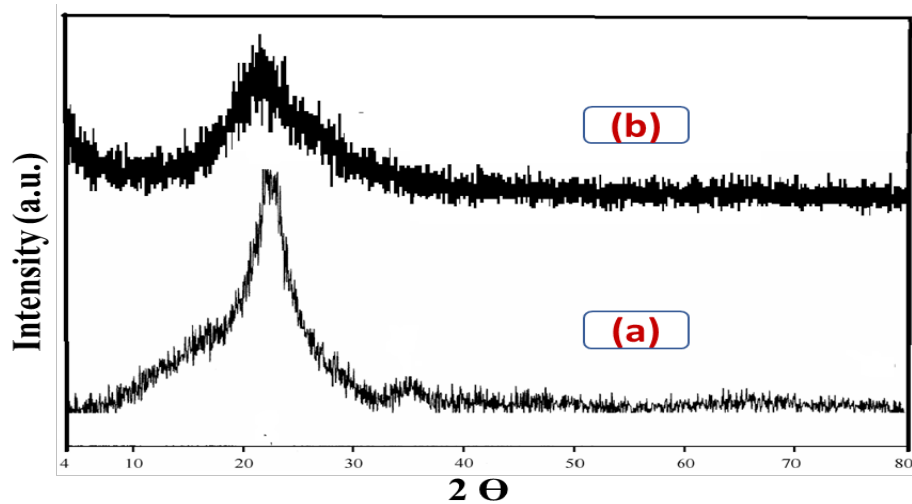


Fig. 1. X-ray diffraction patterns for (a) parent silica and (b) PO<sub>4</sub>/SiO<sub>2</sub>.

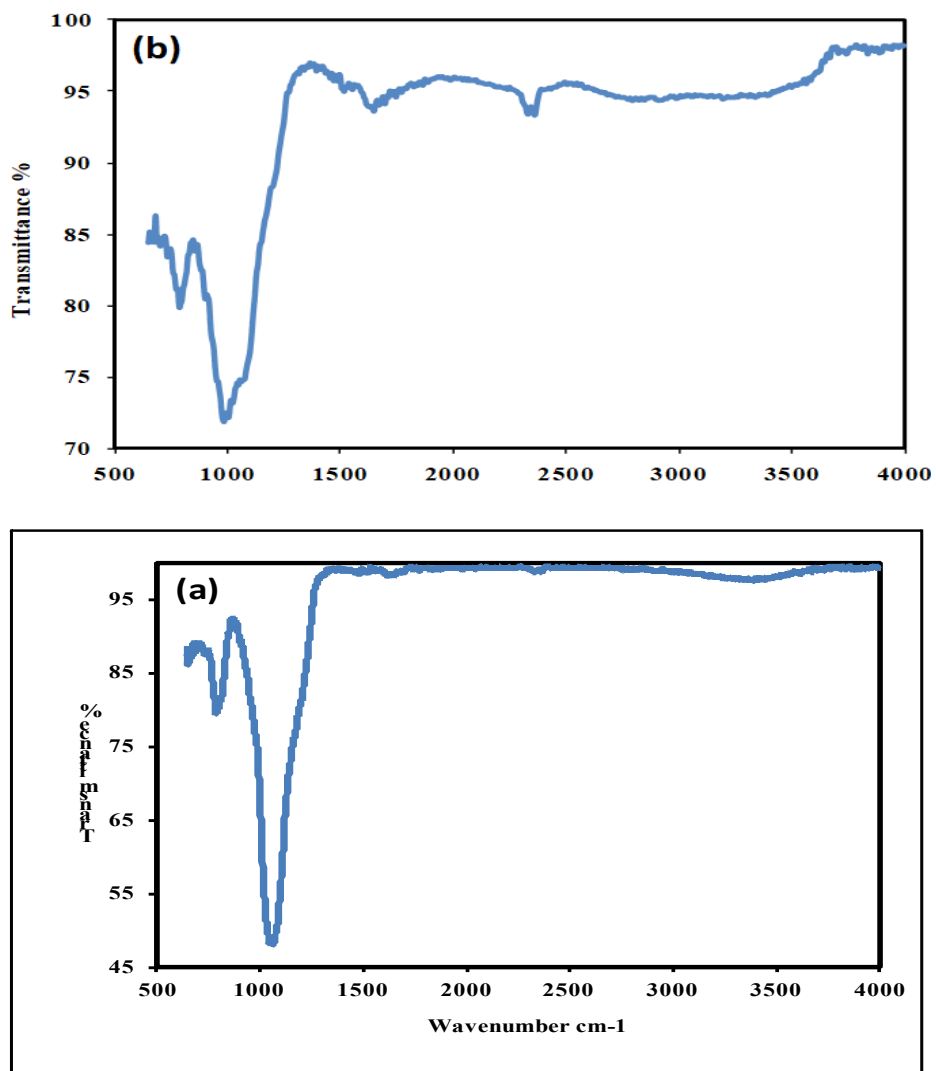


Fig. 2. Infrared spectra of (a) parent silica and (b) PO<sub>4</sub>/SiO<sub>2</sub>.

The nitrogen adsorption isotherm of as-prepared silica and phosphoric acidified silica (Fig. 3) is related to the type IV isotherm according to the IUPAC classification [29], which reveals the existence of the micropores and the macropores in the surface texture. The isotherms are exhibiting H3 hysteresis loop that ended at  $P/P_0 = 0.25$ , which usually associated with the swelling of the non-rigid pores [30]. The BET surface areas of silica and acidified silica samples are 161.9 and 120.5 m<sup>2</sup>/g, respectively (Table 1). The porosity of ex silica created from the pore opening, which takes place during the burning of the rice husk in the air causing the condensation of silanol groups to siloxane bridges. Which is confirms the porosity nature of obtained silica from rice husk [31].

The pore radius distribution (Fig. 4) shows that

the silica contains micropores, which has maxima at about 1.8 nm and narrow mesopores between 2.4 and 4.2 nm. Pores with the large range may be created during silica extraction or due to the presence of enduring voids of tiny particles. While the small ranges were formed during the oxidation process inside the particles [32]. The phosphorous acidified silica exhibits only microspores at about 2.4 nm. Table 1 showed that the surface area decreases from 161.91 to 120.5 m<sup>2</sup>/g, average pore radius from 20 to 13 Å and pore volume from 0.06 to 0.04 cm<sup>3</sup>/g, for parent silica and the acidified silica, respectively. These results attributed to the acidification process and consequently the blocking of the pores by the PO<sub>4</sub> groups. Acetalization of glycerol with a ketone (acetone) is evaluated by the surface acidity of the prepared catalyst since this reaction is keeping on by the presence of acidic nature catalyst.

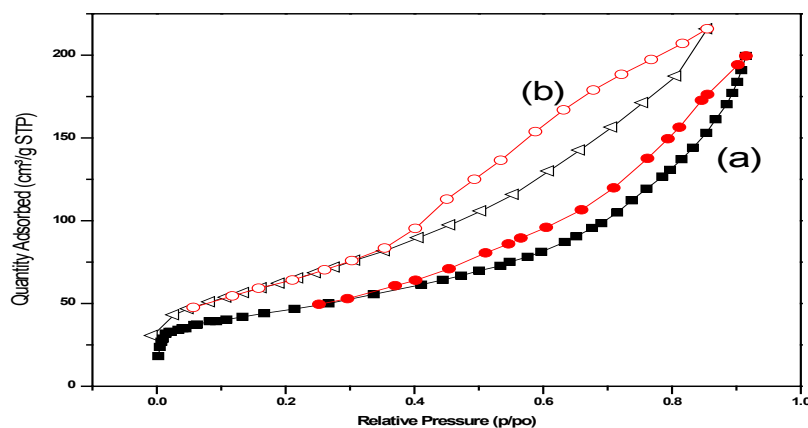


Fig. 3. N<sub>2</sub> adsorption-desorption isotherms of (a) parent silica and (b) PO<sub>4</sub>/SiO<sub>2</sub>.

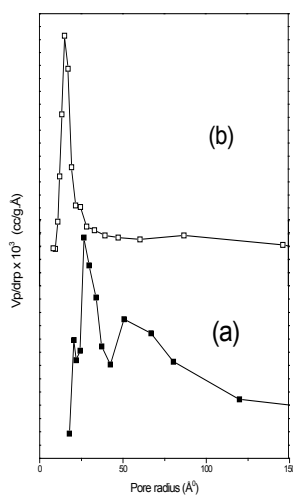


Fig. 4. Pore radius distribution of (a) parent silica and (b) PO<sub>4</sub>/SiO<sub>2</sub>.

The profile of  $\text{NH}_3$ -TPD over the surface of the parent silica sample (Fig. 5.a) showed a little apex around  $400^\circ\text{C}$ , which may be attributed to the existence of acid sites having moderate strength (i.e. silanol groups) [33]. While the phosphate silica showed significant amounts of weak, moderate and strong acid sites that represented by apexes at  $150$ ,  $400$  and  $550^\circ\text{C}$ , respectively [8]. The total amount of the desorbed ammonia was calculated by integrating the areas under the curves and it was found to be  $50$  and  $117 \mu\text{mol NH}_3 \text{ g}^{-1}$  for parent silica and phosphate silica, respectively, which already confirmed by FTIR analysis.

The SEM images of extracted  $\text{SiO}_2$  and  $\text{PO}_4/\text{SiO}_2$  affirmed its porous structure. The  $\text{SiO}_2$  image keeps the outer alleviation of raw RH owing to the layer of surface protective having the regular distribution of  $\text{SiO}_2$ . The walls of the cells located

around and between the pores were destroyed, resulting in the formation of relatively small pores on the heterogeneous surface. During the acidification process ( $\text{PO}_4/\text{SiO}_2$  formation) the well-arranged backbones of rice husk hulls ruined by liberating silica content [31-33]. The smoother surface of the extracted  $\text{SiO}_2$  (Fig. 6a) and porous structure of  $\text{PO}_4/\text{SiO}_2$  (Fig. 6b) affirmed the formation of new fine pores in the later.

#### Catalytic activity

As a reference, a blank reaction had been achieved without catalyst at the optimum conditions, giving negligible results. Moreover, the low acidity of the parent silica (Fig. 5 and Table 1) caused very low conversion of glycerol ( $< 1\%$ ) at the optimum conditions of the reaction, so no more discussion about silica catalytic activity in this paper.

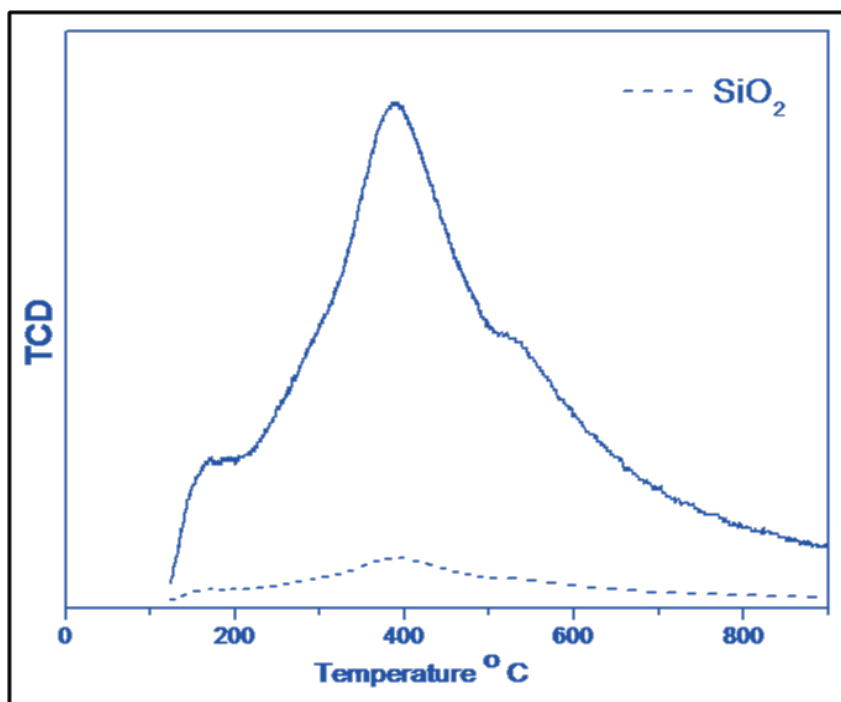


Fig. 5.  $\text{NH}_3$ -TPD profiles of parent silica and  $\text{PO}_4/\text{SiO}_2$ .

TABLE 1. Texture properties of the prepared catalysts.

Sample	$S_{\text{BET}}$ $\text{m}^2/\text{g}$	Average pore radius ( $\text{\AA}$ )	Pore volume $\text{cm}^3/\text{g}$	$\text{NH}_3$ -TPD $\mu\text{mol}$ $\text{NH}_3 \text{ g}^{-1}$	Intrinsic $\mu\text{mol NH}_3/\text{m}^2$
$\text{SiO}_2$	161.91	20	0.04	50	0.3
$\text{PO}_4/\text{SiO}_2$	120.5	13	0.06	117	0.98

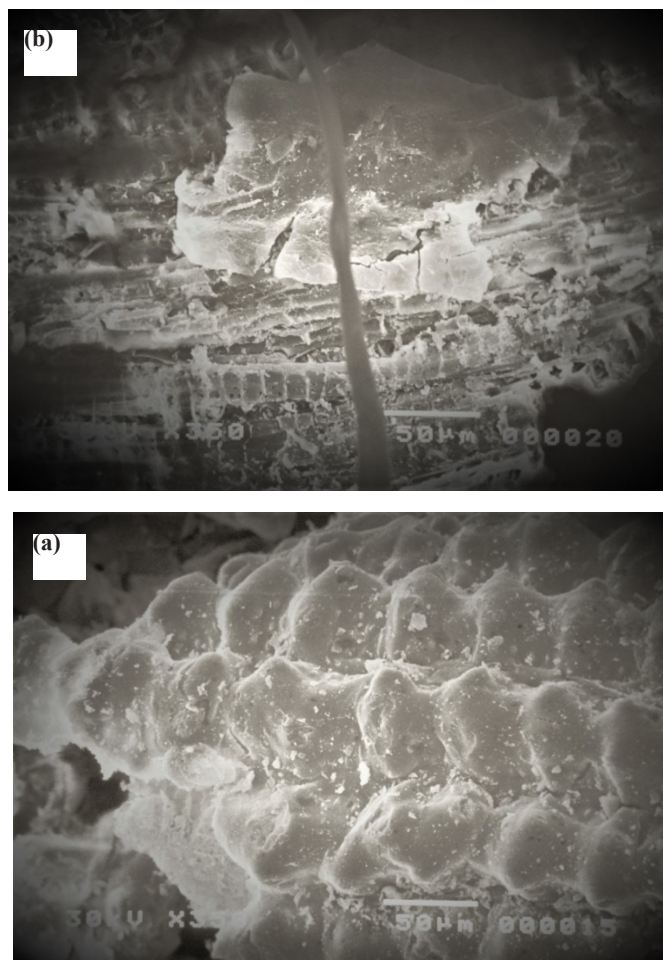


Fig. 6. SEM images of (a) parent silica and (b)  $\text{PO}_4/\text{SiO}_2$ .

Effect of different molar ratio of acetone to glycerol at low temperatures ( $50^\circ\text{C}$ ) was investigated (Fig. 7) in which the total conversion of the reactants decreased from 57.98% to 43.59% by the molar ratio of acetone to glycerol increased from 1:2 to 1:6, while the creation of the solketal (five-membered ring ketal) decreased from 87.95% to 51.32%. On the other hand, the conversion towards the undesired by-products such as six-membered ring acetal, diethyl ether and acetaldehyde increased upon increasing the molar ratio of glycerol: acetone. The previously mentioned selectivity behaviors towards solketal and acetal synthesis associated with decreasing the numbers of reacted moles of glycerol can result from the influence of steric factor [11]. Also, the increasing of the concentration of acetone in the reaction medium may enhance the polarity and consequently directed the conversion towards the six-membered ring acetal [12]. The formation of diethyl ether and acetaldehyde may result from the catalytic cleavage fracture of C-C bond and rearrangement of the hemiketal intermediate [27].

By increasing the reaction temperature from 50 to  $100^\circ\text{C}$  the selectivity of  $\text{PO}_4/\text{SiO}_2$  towards solketal decreased gradually from 87.95% to 73.68% at a low molar ratio of glycerol: acetone = 1:2 (best ratio) indicated the exothermicity of the reaction (Fig. 8) [37]. This catalytic behavior may attribute to the raising of the polarity of the reaction medium due to the removal of the by-product water via vaporization at high temperatures [11]. Also, the variation of the selectivity of the catalyst towards the producing of the different acetals could be explained according to the energy of formation ( $\Delta H_f$ ) of these compounds [11]. The obvious increment in the conversion percentage as the reaction temperature increased may be attributed to increasing the percentages of the undesired by-products diethyl ether and acetaldehyde (Fig. 8). Accordingly, the selected optimum conditions were glycerol to acetone molar ratio = 1:2 and the reaction temperature at  $50^\circ\text{C}$ .

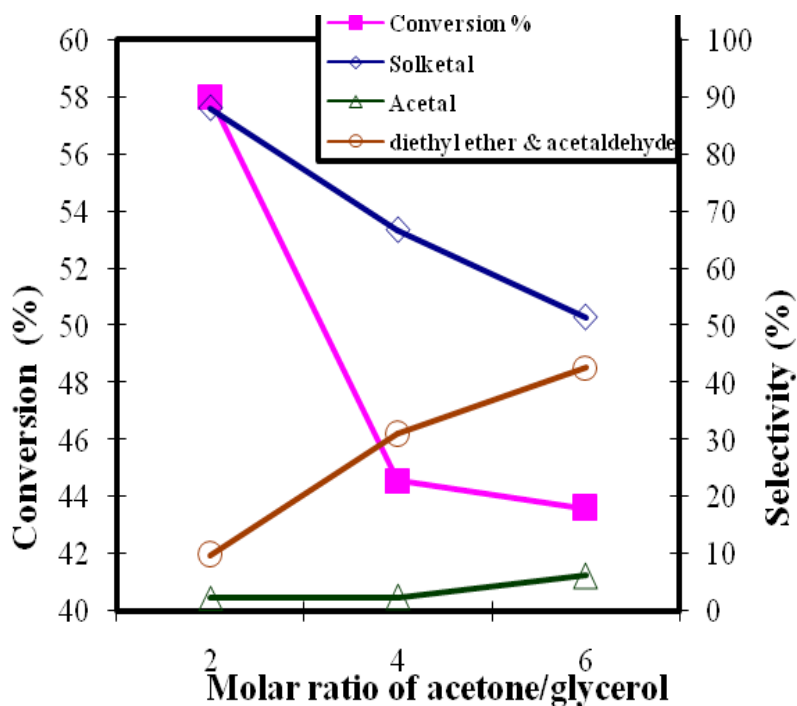


Fig. 7. Effect of acetone to glycerol molar ratio on  $\text{PO}_4/\text{SiO}_2$  catalytic activity. Reaction conditions: catalyst weight: 0.5 g; reaction temperature: 50°C; reaction time: 1 h.

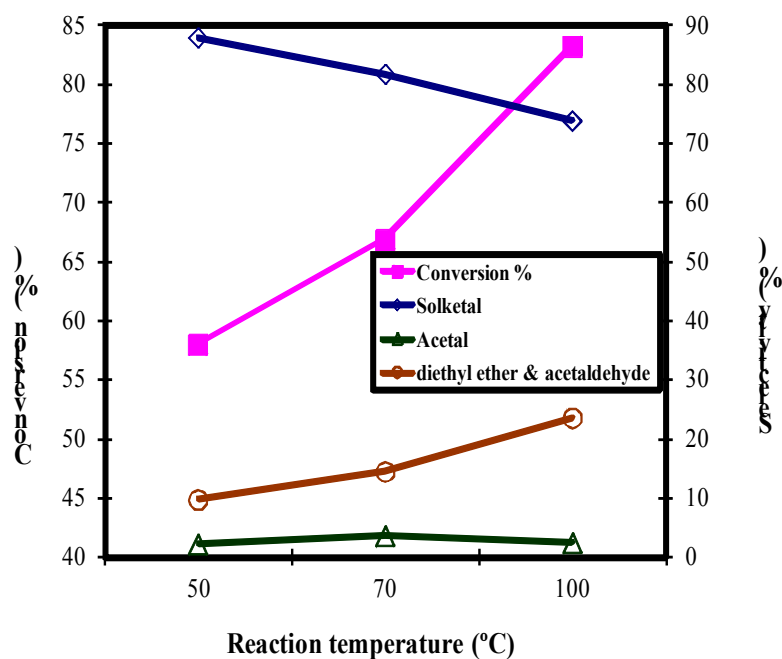


Fig. 8. Effect of reaction temperature on  $\text{PO}_4/\text{SiO}_2$  catalytic activity. Reaction conditions: catalyst weight: 0.5 g; acetone to glycerol molar ratio= 2; reaction time: 1 h.

Figure (9) Showed a gradual increase in the conversion of glycerol upon increasing the quantity of the used catalyst from 100 to 700 mg. Such enhancing in the value of conversion may be owing to the increment of the accessible active spots in the surface of the catalysts as the catalyst amount charged to the reactor increased. These acid sites are responsible for the configuration of the intermediate protonated hemiketal, which transformed into solketal or acetal after dehydration step [11, 14].

The non-significant influence of the amount of the catalyst on its selectivity towards the formation of solketal was previously detected [13]. The selectivity towards solketal slightly decreased as the amount of used catalyst reached 700 mg, that may refer to the increase of the available polar acidic sites and consequently the stabilization of the protonated intermediate,

which is favored conditions for the terminal hydroxyl group nucleophilic attack leading to produce acetal [11].

Figure 10 demonstrated the effect of time on the catalyst performance since it displayed a conversion of glycerol ~76.42% after 1h, and ~90.36% after four hours of reaction time. Afterward, there was no considerable change in the glycerol conversion after 6h (~90.67%). No indications for a deactivation process were observed during experimental tests for up to six hours, which eliminate the possibility of coke deposit formation [28]. In a good agreement with previous reports [11,13], the selectivity of the catalyst towards solketal slightly decreased as the reaction time increased and the selectivity towards acetal increased, which may be attributed to the solketal hydrolysis in presence of the remained by-product water molecules [39].

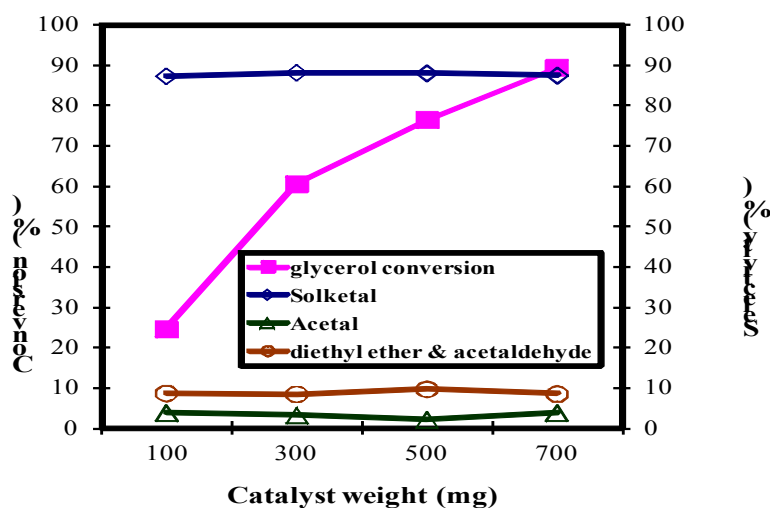


Fig. 9. Effect of catalyst weight on the catalytic activity. Reaction conditions: acetone to glycerol molar ratio= 2; reaction temperature: 50°C; reaction time: 1 h.

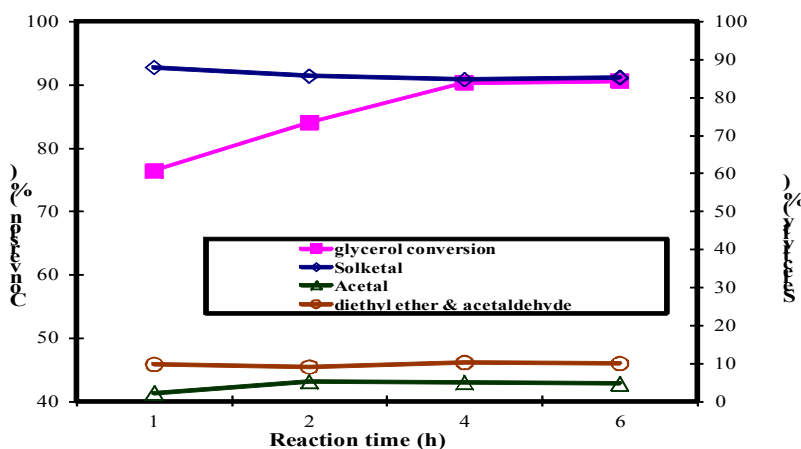


Fig. 10. Effect of reaction time on PO<sub>4</sub>/SiO<sub>2</sub> catalytic activity. Reaction conditions: catalyst weight: 0.5 g; reaction temperature: 50°C; acetone to glycerol molar ratio=2.

In order to study the stability of the catalyst, the reusability test was studied in five subsequent reactions (Fig. 11). As clear, no remarkable change on the conversion and selectivity, this indicates the high stability of the  $\text{PO}_4/\text{SiO}_2$  catalyst.

Table (2) shows the comparison of solketal selectivity towards the acetalization reaction over different catalysts.

### Conclusion

Based on the activity data, pure silica catalyst shows very low activity (less than 1% glycerol conversion) in acetalization reaction due to the very poor acidic properties as indicated by TPD data. While, in the case of  $\text{PO}_4/\text{SiO}_2$  catalyst, the glycerol conversion reached ~90.8%. Two ketals including solketal with a 5-membered

ring (selectivity = 85.24%) and acetal with a 6-membered ring (selectivity = 4.72%) are formed, this relies essentially on the acetalization position contained by the glycerol molecule. The 5-membered ring ketal exhibits lower thermodynamic stability than one with the 6-membered ring. It means that the formation of 5-membered ring ketal is mainly kinetically controlled [7]. This data confirmed that, the catalyst type acting a main role in this reaction, which counts on the strength and type of acid sites [48-51], which are essentially for activation of the carbonyl group of acetone and forming a carbonation that was attacked by the hydroxyl group of glycerol to build up an intermediate which then goes through cyclization by water removing to ketals formation [52]. Moreover, the textural properties of the catalyst (surface area

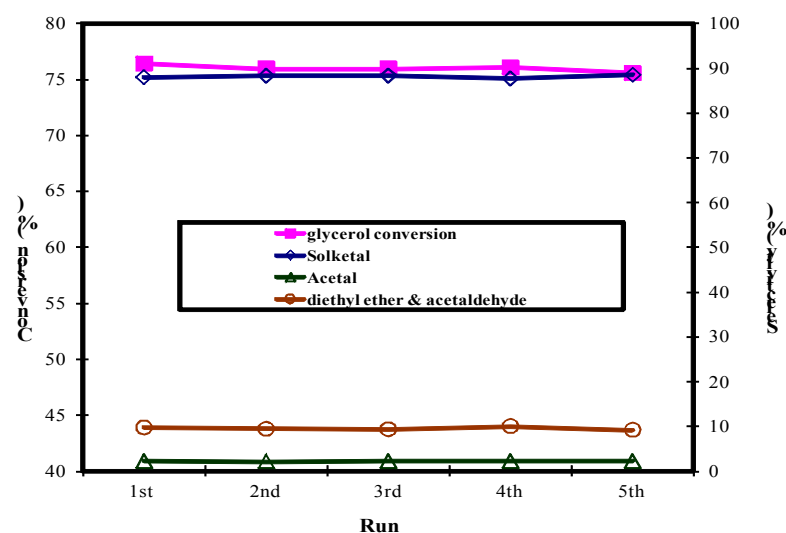


Fig. 11. Reusability of  $\text{PO}_4/\text{SiO}_2$ . Reaction conditions: catalyst weight: 0.5 g; acetone to glycerol molar ratio= 2; reaction temperature: 50°C; reaction time: 1 h.

TABLE 2. Comparison of solketal selectivity by the acetalization reaction over different catalysts.

Catalyst	Solketal Selectivity %	Reference
$\alpha$ -zirconium phosphate	98.6	[40]
Acidic carbon-based catalysts	95	[41]
Algerian acid activated clays	95	[42]
p-Toluenesulfonic acid	98	[43]
silica-included heteropolyacids	98	[44]
Amberlyst – 36 (Wet)	94	[17]
M- $\text{AlPO}_4/x\text{AlPO}_4$ (x = Zn, Cu, Ni, or Co)	75	[18]
MoPO/SBA-15	97	[45]
mesoporous Ni-Zr/AC	75	[46]
$(\text{NH}_4^+ [\text{NbO}(\text{C}_2\text{O}_4)_2(\text{H}_2\text{O})](\text{H}_2\text{O})_n$	65	[47]
$\text{Co}[\text{II}](\text{Co}[\text{III}]_x\text{Al}_{2-x})\text{O}$	98	[48]
<b>Ex- rice husk silica phosphate</b>	<b>90.8</b>	<b>This work</b>

and porosity) are also significant because it assists in the elimination of the diffusion limitation for reactants and products [52]. The optimized conditions of this reaction over 10% PO<sub>4</sub>/SiO<sub>2</sub> to give maximum solketal selectivity are 50°C (lower temperature) and acetone to glycerol molar ratio 2 using a 0.5g catalyst. The catalyst was found to be stable up to more than five cycles.

## References

1. Abu Bakar R., Yahya R., Neon Gan S., Production of High Purity Amorphous Silica from Rice Husk, *Procedia Chem*, **19**, 189 – 195 (2016).
2. Zhang S., Gao H., Li J., Huang Y., Alsaed A., Hayat T., Xu X., Wang X., Rice husks as a sustainable silica source for hierarchical flower-like metal silicate architectures assembled into ultrathin nanosheets for adsorption and catalysis, *J. Hazard. Mater*, **321**, 92–102 (2017).
3. Irzaman I., Dwi Cahyani I., Aminullah A., Maddu A., Yulianto B., Siregar U., Biosilica Properties from Rice Husk using Various HCl Concentrations and Frequency Sources, *Egyptain journal of chemistry*. DOI: 10.21608/EJCHEM.2019.8044.1679.
4. A.M. Rabie, M. Shaban, M.R. Abukhadra, R. Hosny, S.A. Ahmed, N.A. Negm, Diatomite supported by CaO/MgO nanocomposite as heterogeneous catalyst for biodiesel production from waste cooking oil, *Journal of Molecular Liquids*, **279** (2019) 224-231.
5. A.M. Rabie, E.A. Mohammed, N.A. Negm, Feasibility of modified bentonite as acidic heterogeneous catalyst in low temperature catalytic cracking process of biofuel production from nonedible vegetable oils, *Journal of Molecular Liquids*, **254** (2018) 260-266.
6. N.A. Negm, A.M. Rabie, E.A. Mohammed, Molecular interaction of heterogeneous catalyst in catalytic cracking process of vegetable oils: chromatographic and biofuel performance investigation, *Applied Catalysis B: Environmental*, **239** (2018) 36-45.
7. Oprescu E.-E., Stepan E., Dragomir R. E., Radu A., Rosc P., Synthesis and testing of glycerol ketals as components for diesel fuel, *Fuel Process. Technol*, **110**, 214–217 (2013).
8. Zhang S., Zhao Z., Ao Y., Design of highly efficient Zn-, Cu-, Ni- and Co-promoted M-AlPO<sub>4</sub> solid acids: The acetalization of glycerol with acetone, *Appl Catal.*, **496**, 32–39 (2015).
9. Ardila-Suárez C., Rojas-Avellaneda D., Ramirez-Caballero G. E., Effect of Temperature and Catalyst Concentration on Polyglycerol during Synthesis, *Int J Polym. Sc.*, **5**, 1-8(2015).
10. Singh S., Patel A., Selective Green Esterification and Oxidation of Glycerol over 12-Tungstophosphoric Acid Anchored to MCM-48, *Ind. Eng. Chem. Res.*, **53**, 14592–14600 (2014).
11. Khayoon M.S., Hameed B.H., Synthesis of hybrid SBA-15 functionalized with molybdophosphoric acid as efficient catalyst for glycerol esterification to fuel additives, *Appl Catal. A*, **433–434**, 152–161 (2012).
12. Alhanash A., Kozhevnikova E. F., Kozhevnikov I. V., Gas-phase dehydration of glycerol to acrolein catalysed by caesium heteropoly salt, *Appl Catal.*, **A**, **378**, 11–18 (2010).
13. Serafim H., Fonseca I.M., Ramos A.M., Vital J., Castanheiro J.E., Valorization of glycerol into fuel additives over zeolites as catalysts, *Chem. Eng. Sci.*, **178**, 291–296 (2011).
14. Ferreira P, Fonseca IM, Ramos AM, Vital J, Castanheiro JE., Valorisation of glycerol by condensation with acetone over silica-included heteropolyacids, *Appl Catal.*, **B**, **98**, 94–9 (2010).
15. Pandian M., Sanjeev P. Maradur, A.B. Halgeri, Ganapati V. S., Room temperature synthesis of solketal from acetalization of glycerol with acetone: Effect of crystallite size and the role of acidity of beta-zeolite, *J. Mol. Catal. A-Chem.*, **396**, 47–54 (2015).
16. Poirier M-A., Charles C. *J. Mol. Catal. A-Chem.*, A new continuous-flow process for catalytic conversion of glycerol to oxygenated fuel additive: Catalyst screening, *Appl. Energy*, **123**, 75–81 (2014).
17. Nanda MR, Yuan Z, Qin W, Ghaziaskar HS, Poirier M-A, Xu C., Catalytic conversion of glycerol to oxygenated fuel additive in a continuous flow reactor: process optimization, *Fuel*, **128**, 113–119 (2014).
18. Zhang S, Zhao Z, Ao Y., Design of highly efficient Zn-, Cu-, Ni- and Co-promoted M-AlPO<sub>4</sub> solid acids: the acetalization of glycerol with acetone, *Appl Catal A*, **496**, 32–39 (2015).
19. Souza TE, Portilho MF, Souza PMTG, Souza PP, Oliveira LCA., Modified niobium oxyhydroxide catalyst: an acetalization reaction to produce bio-additives for sustainable use of waste glycerol, *Chem Cat Chem*, **6**, 2961–2969 (2014).

20. Khayoon MS, Hameed BH., Acetylation of glycerol to biofuel additives over sulfated activated carbon catalyst, *Bioresour Technol*, **102**, 9229–9235 (2011).
21. Rodrigues R, Goncalves M, Mandelli D, Pescarmona PP, Carvalho WA., Solventfree conversion of glycerol to solketal catalysed by activated carbons functionalised with acid groups, *Catal Sci Technol*, **4**, 2293–2301 (2014).
22. Reddy PS, Sudarsanam P, Mallesham B, Raju G, Reddy BM., Acetalisation of glycerol with acetone over zirconia and promoted zirconia catalysts under mild reaction conditions, *J Ind Eng Chem*, **17**, 377–381 (2011).
23. Fan C-Ni., Xu C-H., Liu C-Q., Huang Z-Y., Liu J-Y., Ye Z-X., Catalytic acetalization of biomass glycerol with acetone over TiO<sub>2</sub>-SiO<sub>2</sub> mixed oxides, *React. Kinet. Mech. Cat.*, **107**, 189–202 (2012).
24. Sudarsanam P., Mallesham B., Prasad A. N., Reddy P. S., Reddy B. M., Synthesis of bio-additive fuels from acetalization of glycerol with benzaldehyde over molybdenum promoted green solid acid catalysts, *Fuel Process. Technol.*, **106**, 539–545(2013).
25. Torres M.D., Jiménez-osés G., Mayoral J.A., Pires E., de los Santos M., Glycerol ketals: Synthesis and profits in biodiesel blends, *Fuel* **94**, 614–616 (2012).
26. Zaki T., Aman D., Catalytic carbon monoxide oxidation over copper/silica nanocatalysts, *Energ. Source. Part A*, **34**, 1923-1932 (2012).
27. Zaki T., Aman D., Preparation and Characterization of Manganese Oxides/Rice Husk Silica Nanosized Catalysts for CO Oxidation, *Energy Sources Part A*, **34**, 2147-2155 (2012).
28. Suprun W., Lutecki M., Haber T., Papp H., Acidic catalysts for the dehydration of glycerol: Activity and deactivation, *J. Mol. Catal. A-Chem.* **309**, 71–78 (2009).
29. Yener H. B., Helvacş. Ş., Effect of synthesis temperature on the structural properties and photocatalytic activity of TiO<sub>2</sub>/SiO<sub>2</sub> composites synthesized using rice husk ash as a SiO<sub>2</sub> source, *Sep Purif Technol.*, **140**, 84–93 (2015).
30. Greeg S.J., Sing K.S.W., adsorption, surface area and porosity, second edition, Academic Press, London, (1982).
31. Lowell S., Shields J.E., Thomas M.A., Thommes M., Characterization of porous solids and powders: surface area, pore size and density, Kluwer Academic Publishers, Netherlands, (2004).
32. James J., Rao M.S., Characterization of silica in rice husk ash, *Am. Ceram. Soc. Bull.*, **65**, 1177-1180 (1986).
33. Liou T-H., Preparation and characterization of nano-structured silica from rice husk, *Mater. Sci. Eng. A.*, **364**, 313–323 (2004).
34. Wua Q., Chena F., Xua Y., Yu Y., Simultaneous removal of cations and anions from waste water by bifunctional mesoporous silica, *Appl. Surf. Sci.* **351**, 155–163 (2015).
35. Ke M., Abdul Wahab J., Hyunsik B., Song K-H., Jung S. L., Mayakrishnan G., Kim I. S., Allantoin-loaded porous silica nanoparticles/polycaprolactone nanofiber composites: fabrication, characterization, and drug release properties, *RSC Adv.*, **6**, 4593-4600 (2016).
36. Shoumkova A., Stoyanova V., SEM–EDX and XRD characterization of zeolite NaA, synthesized from rice husk and aluminium scrap by different procedures for preparation of the initial hydrogel, *J. Porous. Mat.*, **20**, 249-255 (2013).
37. Ferreira P., Fonseca I.M., Ramos A.M., Vital J., Castanheiro J.E., Valorisation of glycerol by condensation with acetone over silica-included heteropolyacids” *Appl. Catal. B: Environ.* **98**, 94-99 (2010).
38. Kima M. , Yoonb S.H. , Choic E., Gild B., Comparison of the adsorbent performance between rice hull ash and rice hull silica gel according to their structural differences, *LWT* **41**, 701–706 (2008).
39. Ozorio L.P., Pianzolli R., Motaa M.B.S., Mota C.J. A., Reactivity of Glycerol/Acetone Ketal (Solketal) and Glycerol/Formaldehyde Acetals toward Acid-Catalyzed Hydrolysis, *J. Braz. Chem. Soc.* **23**, 931-937 (2012).
40. Xuewen L. , Yuanyuan J. , Ruru Z. , Zhaoyin H., Layered  $\alpha$ -zirconium phosphate: An efficient catalyst for the synthesis of solketal from glycerol, *Applied Clay Science*, **174**, 120–126 (2019).
41. Maraisa G., Raphael R. , Thalita S. G. , Wagner A. C., Highly selective acetalization of glycerol with acetone to solketal over acidic carbon-based catalysts from biodiesel waste, *Fuel* **181**, 46–54 (2016).

42. Kouider A., Fouad L., Sondes A., Ali R., Ezzedine S., Néji B., Algerian Acid Activated Clays as Efficient Catalysts for a Green Synthesis of Solketal by Chemoselective Acetalization of Glycerol with Acetone, *Bulletin of Chemical Reaction Engineering & Catalysis*, **14** (1), 130-141 (2019).
43. Mushrush GW, Hardy D., Fuel system icing inhibitor and deicing composition. Patent US5705087 A; 1998.
44. Sailaja G., PethanRajan N., Srinivasa Rao and Komandur G., Chary V. R., Acetalization of Glycerol with Acetone to Bio Fuel Additives over Supported Molybdenum Phosphate Catalysts, *Journal of Molecular Catalysis A: Chemical*, (2015).
45. Khayoon M.S., Hameed B.H., Solventless acetalization of glycerol with acetone to fuel oxygenates over Ni-Zr supported on mesoporous activated carbon catalyst, *Applied Catalysis A: General* **464** – **465**, 191–199 (2013).
46. Talita E. S., Marcio F. P., Priscila M. T. G. S., Patterson P. S., Luiz C. A. O., Modified Niobium Oxyhydroxide Catalyst: An Acetalization Reaction to Produce Bio-additives for Sustainable Use of Waste Glycerol, *Chem Cat Chem*, **6**, 2961 – 2969 (2014).
47. Xuewen Li, Liping Z., Zhaoyin H., Acetalization of glycerol with acetone over Co[II](Co[III]<sub>x</sub>Al<sub>2-x</sub>)O<sub>4</sub> derived from layered double hydroxide, *Fuel* **233**, 565–571(2018).
48. Li L., Koranyi T.I., Sels B.F., Pescarmona P.P., Highly-efficient conversion of glycerol to solketal over heterogeneous Lewis acid catalysts, *Green Chem.*, **14**, 1611–1619 (2012).
49. Manjunathan P., Maradur S.P., Halgeri A.B., Shanbhagi G.V., Room temperature synthesis of solketal from acetalization of glycerol with acetone: Effect of crystallite size and the role of acidity of beta zeolite, *J. Mol. Catal. A: Chem.* **396**, 47–54 (2015).
50. Nanda M. R., Yuan Z., Qin W., Ghaziaskar H. S., Poirier M-A., Xu C. C., Thermodynamic and kinetic studies of a catalytic process to convert glycerol into solketal as an oxygenated fuel additive, *Fuel*, **117**, 470–477 (2014).
51. Rodrigues R., Gonçalves M., Mandelli D., Pescarmona P.P., Carvalho W.A., Solvent-free conversion of glycerol to solketal catalysed by activated carbons functionalised with acid groups, *Catal. Sci. Technol.*, **4**, 2293-2301 (2014).
52. Sandesh S., Halgeri A.B., Shanbhag G.V., Utilization of renewable resources: Condensation of glycerol with acetone at room temperature catalyzed by organic-inorganic hybrid catalyst, *J. Mol. Catal. A-Chem.*, **401**, 73–80 (2015).

### تأثير أيون الفوسفات على محفز السيليكا الحيوي على التركيب الوقود النظيف

داليا رضوان<sup>1</sup>، تامر زكي<sup>2</sup>، هويدا عبد السلام<sup>3</sup>، دلفين أمان<sup>1</sup>  
<sup>1</sup>قسم التكرير - المعهد المصري لأبحاث البترول (EPRI) - مدينة نصر - صندوق بريد ١١٧٢٧ - القاهرة - مصر  
<sup>2</sup>مركز تكنولوجيا النانو - المعهد المصري لبحوث البترول - مدينة نصر - صندوق بريد ١١٧٢٧ - القاهرة - مصر  
<sup>3</sup>قسم التحليل والتقييم - المعهد المصري لبحوث البترول - مدينة نصر - صندوق بريد ١١٧٢٧ - القاهرة - مصر

يمكن إنتاج solketal المضاف للوقود من خلال تفاعل استسقاء منتج ثانوي للديزل الحيوي (الجلسرين) والأسيتون. أجري هذا التفاعل على السيليكا المحمضة المشتقة من قشر الأرز المستدام كمصدر طبيعي بيئي في مفاعل بدون مذيب. وتمت دراسة الخواص الكيميائية والهيكلية للمحفز المحضر بواسطة حيود الأشعة السينية، يحول فورييه مطيافية الأشعة تحت الحمراء والأيزوثيرم الامتزاز / الامتزاز، درجة الحرارة المبرمجة الامتزاز من الأمونيا ومسح المجهر الإلكتروني استنادا إلى هذه الورقة، فإن الظروف الأمثل باستخدام حمض الفوسفوريك حمض 15٪ المستخرجة من قشر الأرز هي 50 درجة مئوية (انخفاض درجة الحرارة) مع النسبة المولية للأسيتون: الجلسرين = 2. يستخدم اختبار قابلية إعادة الاستخدام لفحص ثبات تم التحقيق في النشاط الحفاز. هذا الجهد هو خطوة خطيرة للتنمية والتفكك من solketal كمنتج رئيسي من الجلسرين والأسيتون باستخدام موارد النفايات.